Oceanological and Hydrobiological Studies

International Journal of Oceanography and Hydrobiology

Volume 54, No. 4 December 2025
pages (380-391)

ISSN 1730-413X
eISSN 1897-3191

Experimental observations on ultrastructure of scales of red seabream (*Pagrosomus major*) for seawater pH monitoring

by

Weili Hou[1,2,a], Li Tian[1,b,*], Xin Sun[1,c], Xin Li[1,d], Xiangming Chen[1,e], Haijun Song[1,f]

DOI: **https://doi.org/10.26881/oahs-2025.1.29**
Category: **Original research papers**
Received: **June 01, 2025**
Accepted: **December 08, 2025**

[1]*State Key Laboratory of Geomicrobiology and Environmental changes, China University of Geosciences (Wuhan), Wuhan 430074, Hubei Province, China*

[2]*School of Environmental Studies, China University of Geosciences (Wuhan), Wuhan 430074, Hubei Province, China*

[a] *(https://orcid.org/0009-0000-3383-8289)*
[b] *(https://orcid.org/0000-0003-3005-2007)*
[c] *(https://orcid.org/0009-0009-7242-1772)*
[d] *(https://orcid.org/0009-0003-4213-8702)*
[e] *(https://orcid.org/0000-0003-1901-0359)*
[f] *(https://orcid.org/0000-0002-2721-3626)*

* Corresponding author: *tianlibgeg@cug.edu.cn*

Abstract

Ocean acidification monitoring relies predominantly on field test and numerical modeling, while bioindicators are emerging as practical and economic approaches for seawater pH monitoring. Here, we report indoor dissolution experiments on the scale of red seabream (*Pagrosomus major*) under varied pH (from 7.1 to 7.9), showing that the mean aspect ratio of ventral ctenii and caudal/ventral lepidonts negatively correlated with pH. We propose to employ these ultrastructures of fish scale to be a novel bioindicator for marine pH reconstruction. This semiquantitative proxy would be applicable to both contemporary biomonitoring and paleo-oceanic pH reconstruction for the extensive occurrences of fish in modern oceans and fossil records.

Key words: fish scale, bioindicator, ocean acidification, ultrastructure

1. Introduction

Ocean acidification refers to the progressive decline in seawater pH caused by the oceanic absorption of anthropogenic CO_2 (Gattuso & Hansson, 2011). The global ocean has sequestered enormous anthropogenically emitted CO_2 since the pre-industrial era (Liu & Xie, 2017; Sabine et al., 2004), driving a 0.1 pH decline in global surface oceans (Caldeira & Wickett, 2003). While this pH shift seems to be numerically modest, it corresponds to a ~30% increase in hydrogen ion concentration ($[H^+]$), representing significant acidification of seawater (Iglesias-Rodriguez, 2012). Such contemporary ocean acidification has occurred 100-fold faster than natural background pH variability over the past 650 000 years (Ní Longphuirt et al., 2010; Ridgwell & Schmidt, 2010; Solomon et al., 2007). Under IPCC (The Intergovernmental Panel on Climate Change)-projected emission trajectories, surface ocean pH could decrease to 0.3–0.5 units below pre-industrial values by 2100 (Caldeira & Wickett, 2005). For unmitigated emission scenarios, oceanic surface pH might reach 0.7 units by 2300 (Zeebe et al., 2008).

Ocean acidification affects all marine zones from abyssal plains to littoral ecosystems (Feely et al., 2009, 2010; Orr et al., 2005), exerting pervasive impacts on marine biota (Doney et al., 2009). Acidification disrupts biomineralization pathways and enhances skeletal decalcification in shell-forming mollusks (e.g., oysters) and scleractinian corals that biosecrete calcium carbonate structures (NOAA, 2025). Under acidified conditions, planktonic calcifies (coccolithophores/foraminifera) experience reduced calcification rates, potentially changing trophic networks and ecosystem functions (Cooley & Doney, 2009; Silverman et al., 2009). Given ocean acidification's substantial marine biosphere and ecosystems impact, pH monitoring constitutes a critical task addressing climate change presently. Over the past two decades, moored buoys equipped with instruments and data loggers have been deployed globally (Marshall et al., 2019). These monitoring stations capture long-term variations in seawater chemistry, and provide spatially discrete data, but their implementation and maintenance incur substantial costs (Marshall et al., 2019). Biomonitoring provides a cost-effective supplementary methodology for coastal acidification assessment (Gaylord et al., 2018; Miller et al., 2023).

Fish is one of the major animal groups of aquatic fauna, playing key roles in marine ecosystems (Rishi & Jain, 1998). Fish scales are located on the exterior surface of the body, providing physical protection against predators and parasites, preventing surface fouling, and modifying flow during swimming (Wainwright & Lauder, 2018). Scale morphology exhibits strong potential as an effective bioindicator of aquatic pollution since they continuously interact with waterborne pollutants (Rishi & Jain, 1998). Ultrastructural morphological changes in scales can serve as early signs of trace-level dye exposure stresses, while even the scales of deceased fish may be applicable for reconstruction environmental changes preceding mortality (Kaur et al., 2016). Utilizing alterations in fish scale morphology as bioindicators for climatic and environmental changes offers the additional advantage of enabling non-destructive sampling, since there is no need to sacrifice animals.

This study quantifies pH-dependent microstructural variations in scales of an extensive distributed economic fish, the red seabream (*Pagrosomus major*), which is widespread in the Pacific and Indian oceans, to establish a potential new pH bioindicator.

2. Materials and methods

The red seabream (*P. major*) is one of the most important marine fish species in the aquaculture industries of eastern Asia, with a broad distribution across coastal areas of the Pacific and Indian oceans (approximately 34°N–15°N), prized for its flavor and health-related dietary qualities (Cai et al., 2014; Sarker et al., 2005). Morphologically, (1) it has an oblong–oval and laterally compressed body adorned with numerous blue spots when fresh; (2) its body is relatively shallow, with body depth being two or more times as the standard body length; (3) it possesses 6.5–7 scale rows between the lateral line and dorsal fin origin; (4) all dorsal fin spines are robust and not elongated; and (5) the caudal fin has a black posterior margin and a white lower margin (Bergstad, 1991). It typically lives at depths of 10–50 m, often over both rough and soft substrates (Frimodt, 1995). Adults migrate into shallower parts of their depth range to spawn in late spring and summer, while juveniles are mainly found in shallower areas, preying on benthic invertebrates, including echinoderms, worms, mollusks, and crustaceans and fishes (Frimodt, 1995).

To analyze scale ultrastructure in red seabream (*P. major*), specimens were sourced from coastal markets in the Zhoushan region in October 2023. The Zhoushan Sea area (29°32′–31°04′ N, 121°30′–123°25′ E) is bordered by the Yangtze River Estuary to the north, Hangzhou Bay to the west, and the broad East China Sea continental shelf to the east, consisting of dense islands, located within a subtropical monsoon climate zone known for its strong seasonality (Fu et al., 2019).

The region hosts China's largest fishing ground and several national-level marine ranches (Xiao et al., 2024). The maximum depth of the regional onshore shelf is approximately 50 m, with most areas shallower than 20 m (Wang et al., 2025), while the average annual salinity ranges from 6.72 to 32.62, and the pH ranges from 8.03 to 8.45 (Li et al., 2024).

Scales were collected from caudal, ventral, and dorsal regions (Figure 1) using fine-tipped forceps, picking up 10 scales per part and followed by gentle rinsing in pure water. Samples were immersed in flow-through aquarium systems with seawater maintained at four pH levels: 7.04 ± 0.10, 7.31 ± 0.10, 7.45 ± 0.05, 7.67 ± 0.06, and 7.86 ± 0.05. Water mass pHs were maintained through controlled CO_2 dosing and calcium reactor systems (AQUA EXCEL) to preserve carbonate equilibria. The calcium reactor adjusts and controls factors such as CO_2 gas, water flow, and calcium-alkaline media to facilitate reactions between dissolved carbon dioxide and alkaline substances in the water. This process precipitates calcium ions while generating a calcium bicarbonate solution, which supplies essential calcium and alkaline ions for aquarium organisms, promotes water stability and biological reproduction, and lowers pH levels by increasing dissolved CO_2 concentration through controlled gas infusion. The pH was continuously monitored and regulated using a pH controller (Weipro PH-2010, WEIPRO) until the target values were achieved and stabilized. The experiment was conducted from 6 November 2023, to 18 January 2024, as the temperature of aquarium maintains 25 ± 0.3°C. Relevant parameters are summarized in Table 1.

The pure water cleaned fish scales were air-dried at ambient conditions. To prevent structural curling, the scales were flattened and secured between glass slides for 48 hr and 72 hr prior to microscopic observations. The dried scales were mounted on metal stubs using double-sided adhesive tape, with their front side facing upward

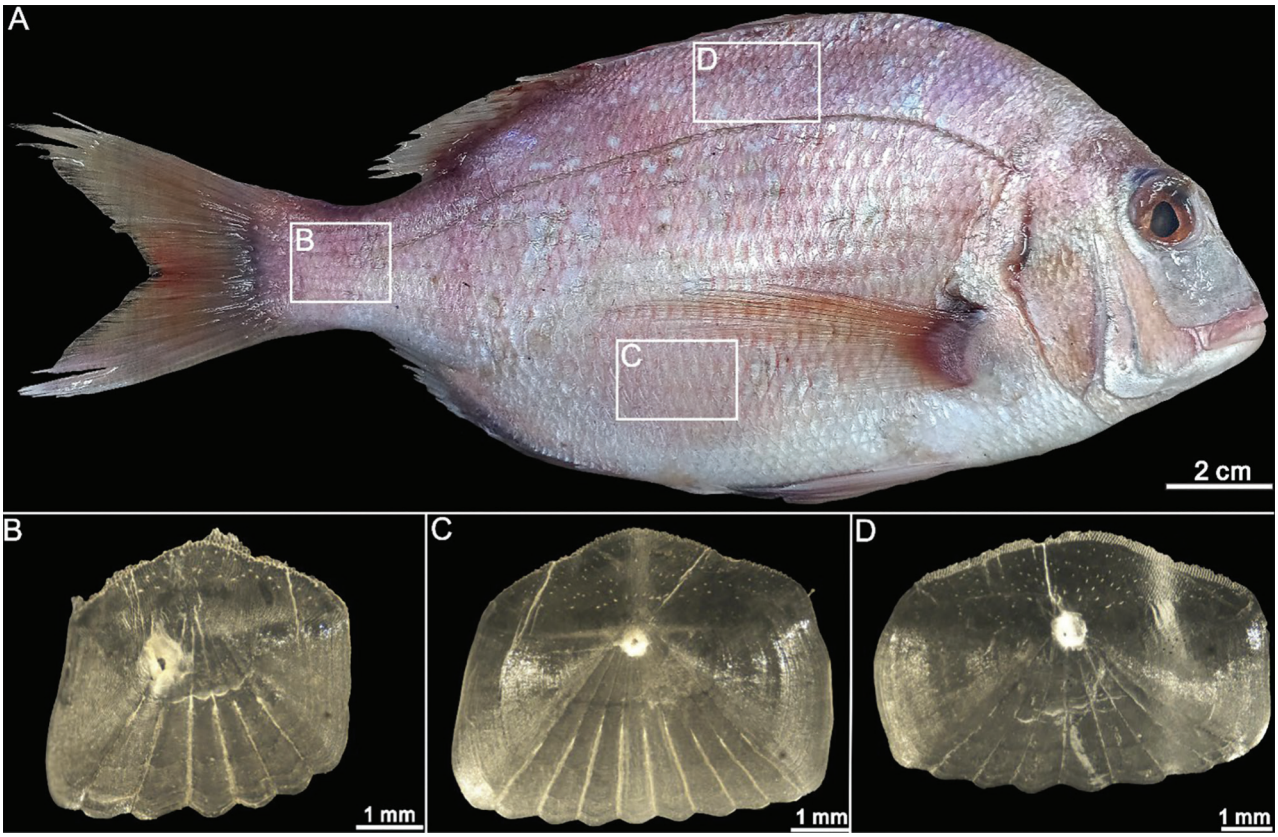

Figure 1

Overall view of sea bream (*P. major*) and morphology of caudal, ventral, and dorsal scales under stereomicroscopy. **(A)** Schematic diagram depicting three distinct anatomical regions of scale removal from the left lateral side of the red seabream (*P. major*). **(B–D)** Photomicrographs of scales from the caudal (tail), ventral (abdominal), and dorsal (back) regions, respectively, obtained via optical microscopy.

Table 1

Seawater carbonate chemistry parameters at different pH levels.

	Measured				Calculated		
pH_N	pH_T	TA (µmol kg−1)	T (°C)	S (PSU‰)	pCO_2 (µatm)	Ω_{calc}	Ω_{arag}
7.9	7.86 ± 0.05	2305.71 ± 255.73	24.97 ± 0.40	30.55 ± 0.79	667.37 ± 117.96	3.55 ± 0.68	2.32 ± 0.44
7.7	7.67 ± 0.06	2269.71 ± 225.08	24.96 ± 0.44	30.21 ± 0.77	1100.05 ± 185.49	2.34 ± 0.5	1.53 ± 0.32
7.5	7.45 ± 0.05	2311.86 ± 235.12	25.12 ± 0.41	30.35 ± 0.76	1936.22 ± 307.07	1.5 ± 0.31	0.98 ± 0.2
7.3	7.26 ± 0.06	2368.09 ± 252.74	24.97 ± 0.43	30.71 ± 0.93	3075.08 ± 504.82	1.04 ± 0.27	0.68 ± 0.17
7.1	7.04 ± 0.10	2342.55 ± 411.40	24.97 ± 0.43	30.31 ± 1.20	5538.39 ± 1423.63	0.63 ± 0.21	0.41 ± 0.14

pH, total alkalinity, temperature, and salinity were measured. pCO_2, DIC, Ωcalc, and Ωarag were calculated using the CO2SYS program. Values are expressed as mean ± SD.
SD, standard deviation. TA, total alkalinity. PSU, practical salinity unit(‰).

and the rear side adhered to the tape. Scale morphology and ultrastructure were analyzed using stereomicroscopy (ZEISS Stemi 305, Zeiss) and field-emission scanning electron microscopy (SEM; Hitachi SU8010, HITACHI). A 30 nm thick gold film was applied to the samples using a sputter coater (Quorum Q150T PLUS, QUORUM). This gold coating effectively mitigated charging effects and beam damage during imaging, and enhanced secondary electron signal intensity from the sample surface. The scales were observed under high vacuum in a scanning electron microscope (SEM) with the following parameters: an accelerating voltage of 15/3/5 kV and a low probe current.

Microstructural features were systematically archived through digital image acquisition, with particular emphasis on ctenii and lepidont architectures. Typically, the most visible portion of the scale (referred to as the posterior field) is composed of interlocking ctenii. In such cases, only the rearmost one or two rows of ctenii remain fully developed spines, whereas older ctenii are reduced to shortened, interlocking stubs (Lanzing & Higginbotham, 1974). Lepidont functions as hooks that anchor the scales to the dermis, securing their position and preventing them from loosening or detaching from the fish. Additionally, they act as friction pads between the anterior portion of the scale and the posterior overlapping scales, aiding in movement (Khanna et al., 2007).

The measurement aspect ratios (length-to-width) of ctenus and lepidont were visualized by using Origin (2025). Specific measurement methodologies are detailed in Figures 2D and 2E. Box plot distribution patterns revealed significant linear associations between ventral ctenii and caudal/ventral lepidont microstructural parameters with environmental pH gradients, prompting the implementation of Pearson correlation analysis to quantify these pH-dependent structural relationships.

3. Results

Variations are found in scale morphology of this fish in different body parts (Figure 1). The ctenii are arranged in an interlocking pattern within the posterior field (Figures 2A,B). In their natural state, they possess elongated and intact tips, and with slightly rectangular segments (Figure 2B). Lepidonts protrude from the circuli, with adjacent lepidonts spaced 0.002 mm apart and exhibiting a conical shape (Figure 2C). Morphological variability is also observed in lepidont forms, including blunt, pointed, acute, short, or truncated morphotypes (Echreshavi et al., 2023; Figure 2C).

Compared with the control group, the ctenial tips in the experimental groups (caudal, ventral, and dorsal scales) exhibited significant shortening, whereas the overall arrangement of ctenii remained morphologically intact (Figure 3). The patterns of tip damage varied: parts of ctenii displayed smooth-edged notches (Figure 3B), others showed localized pitting (Figure 3D), and even partial reduction in interfacial contact area between adjacent ctenii, resulting in loosened structural integration (Figure 3N). Meanwhile, the dorsal lepidonts exhibited sparser spacing between adjacent structures (Figure 4). Relative to the control group, all experimental groups (caudal, ventral, and dorsal) displayed lepidont tip shortening (Figure 4), though the degree of shortening and the morphology of apical notches varied. Partial lepidonts were blunted (Figure 4B), others showed beveled tips with partial truncation (e.g., Figure 4I), and the remaining lepidonts developed surface pitting (Figure 4J).

As shown in Figure 5, the average length-to-width ratio of ctenii of caudal scales under pH 7.1, 7.5, 7.7, and 7.9 conditions is 1.009 (Aspect Ratio = 0.81–1.18),1.005 (AR = 0.84–1.11), 0.978 (AR = 0.83–1.18), and 1.001 (AR = 0.81–1.19), respectively; while those of ctenii of ventral scales are 1.237 (AR = 1.05–1.32), 1.328

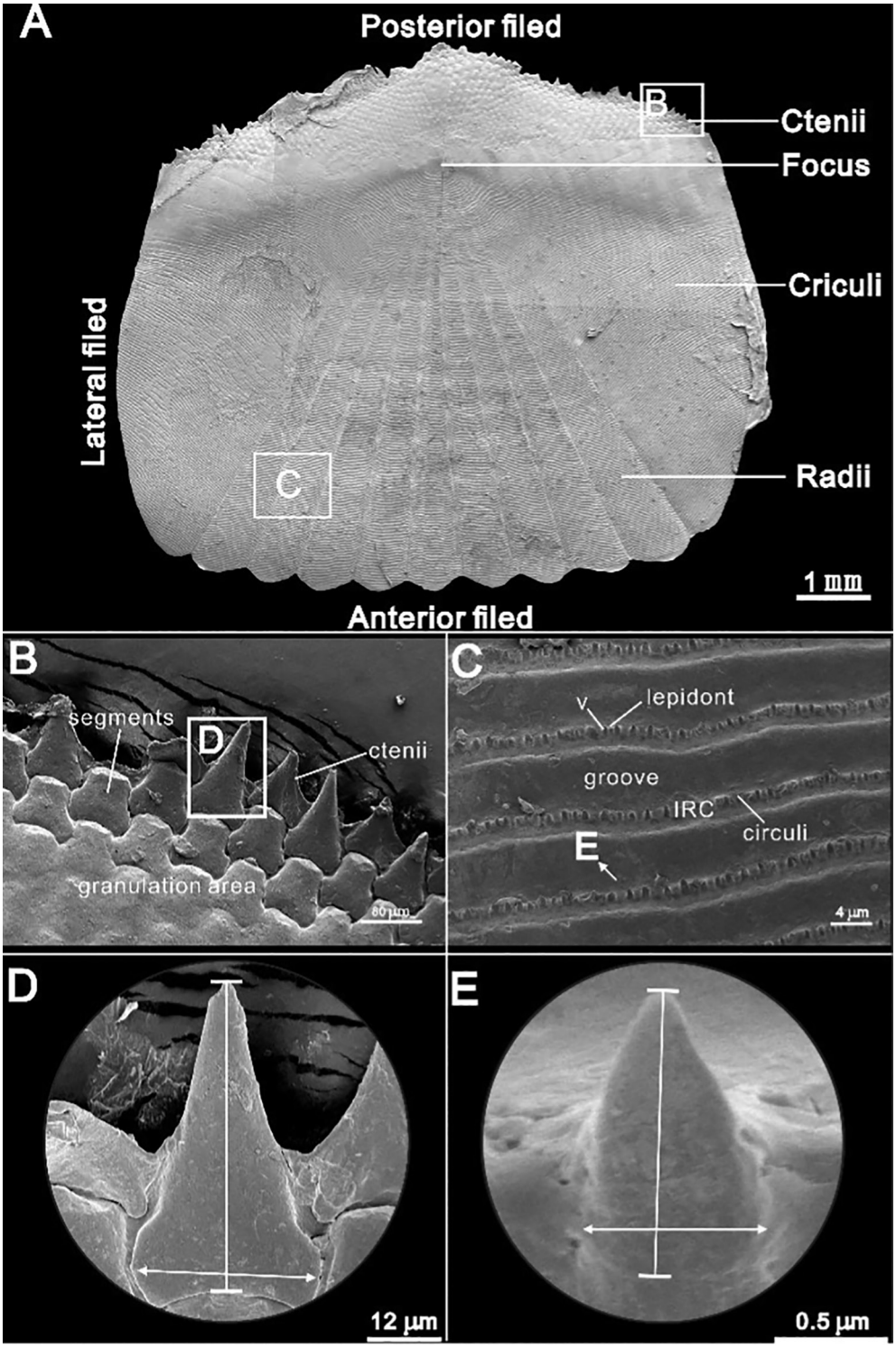

Figure 2

Fish scale structures at different scales under FE-SEM. **(A)** Morphological terminology of the scale. **(B,C)** Focused areas of the anterior field and posterior field under scanning electron microscopy (SEM), respectively. **(D,E)** Schematic diagrams of the measurement scale, illustrating the methodologies for quantifying the longitudinal and basal transverse dimensions of the microstructural components ctenii and lepidont, respectively. FE-SEM, field emission scanning electron microscopy.

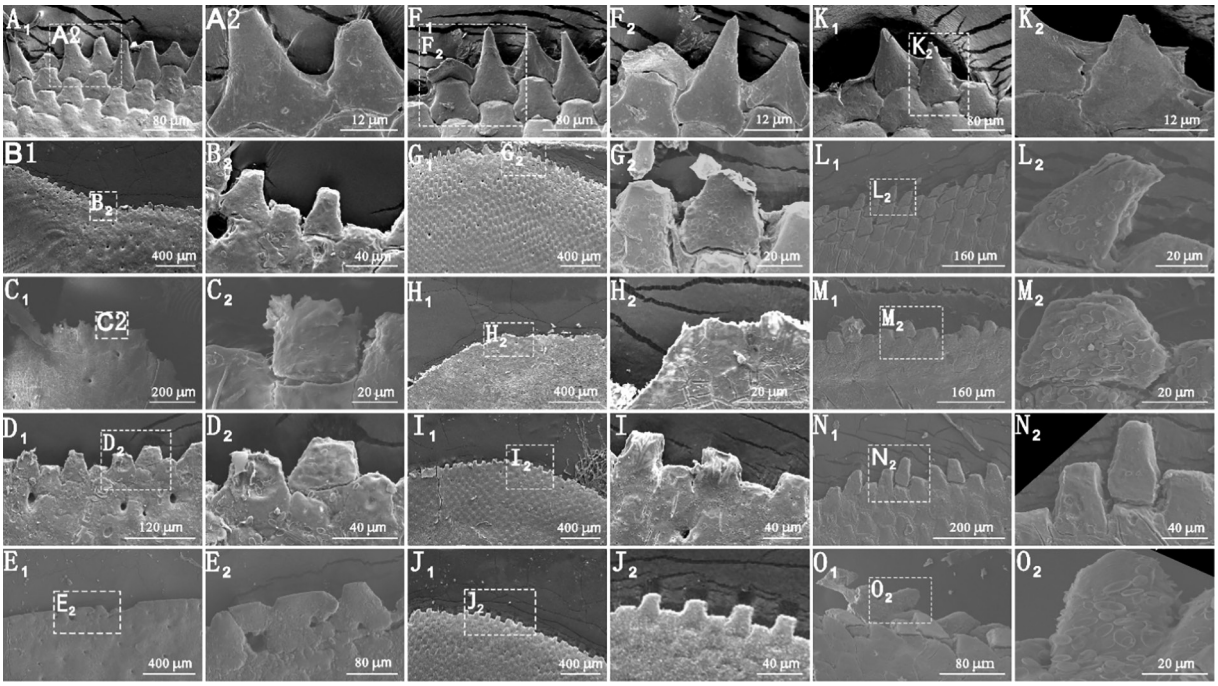

Figure 3

FE-SEM analysis of ctenii ultrastructures in scales from different body regions (caudal, ventral, dorsal). From left to right: FE-SEM images of the ctenii regions in scales from the caudal (tail), ventral (abdomen), and dorsal (back) regions of red seabream (*P. major*). **(A,F,K)** Untreated control scales from the three respective body regions. **(B–E)** FE-SEM images of caudal scales exposed to experimental aquaria with pH levels of 7.1, 7.5, 7.7, and 7.9, respectively. (G–J, L–O) Correspond to FE-SEM images of ventral scales and dorsal scales under identical pH treatments, respectively. FE-SEM, field emission scanning electron microscopy.

(AR = 1.15–1.65), 1.071 (AR = 0.92–1.15), and 0.887 (AR = 0.75–1.12); and those of ctenii of dorsal scales are 1.452 (AR = 1.16–1.64), 0.982 (AR = 0.71–1.22), 1.279 (AR = 1.15–1.51), and 1.230 (AR = 0.70–1.70). The average length-to-width ratio of the lepidont of caudal scales under pH 7.1, 7.5, 7.7, and 7.9 conditions is 0.885 (AR = 0.63–1.13), 1.271 (AR = 0.74–1.63), 1.134 (AR = 1.52–1.81), and 0.922 (AR = 0.75–1.08), respectively; while the lepidont ratios of the ventral scales are 0.596 (AR = 0.35–0.85), 1.731 (AR = 1.05–1.52), 1.117 (AR = 0.53–0.68), and 0.619 (AR = 0.25–0.63); and the lepidont ratios of the dorsal scales are 0.329 (AR = 0.13–0.38), 1.022 (AR = 0.55–1.43), 0.346 (AR = 0.21–0.42), and 1.048 (AR = 0.75–1.48). It is worth noting that the data for pH 7.3 is absent for the unexpected serve sample fragmentation due to the broken water-mass circulation system.

4. Discussion

Acidic conditions induce microstructural erosion at ctenii/lepidont apices (Figures 3 and 4), attributable to calcium dissolution and collagen degradation, thereby compromising scale integrity. Fish scales are composed of two distinct layers: a rigid upper mineralized layer consisting of calcium phosphate (hydroxyapatite) and a poorly mineralized layer (referred to as the basal plate or fibrous plate) primarily made of collagen (Fouda, 1979; Hutchinson and Trueman, 2006; Zylberberg, 2004; Zylberberg & Nicolas, 1982). The well-mineralized outer layer of bony scales is composed of thin collagen fibrils embedded within a mineral crystal matrix, but lacks thicker collagen fibers (Zylberberg, 2004; Zylberberg & Nicolas, 1982). The basal plate is composed of continuous collagen layers arranged in a lamellar manner, approximately 100 nm in diameter (Zylberberg, 2004). The orientation of these fiber shifts from one layer to the next, form a plywood-like structure (Weiner & Wagner, 1998; Zylberberg, 1988). Notably, the ultrastructure of fish scales is influenced by variations in physicochemical factors such as ionic concentrations in water, exposure duration, temperature, and salinity. Compared with ctenii, lepidonts exhibit a more pronounced response to pH changes—even though the dorsal

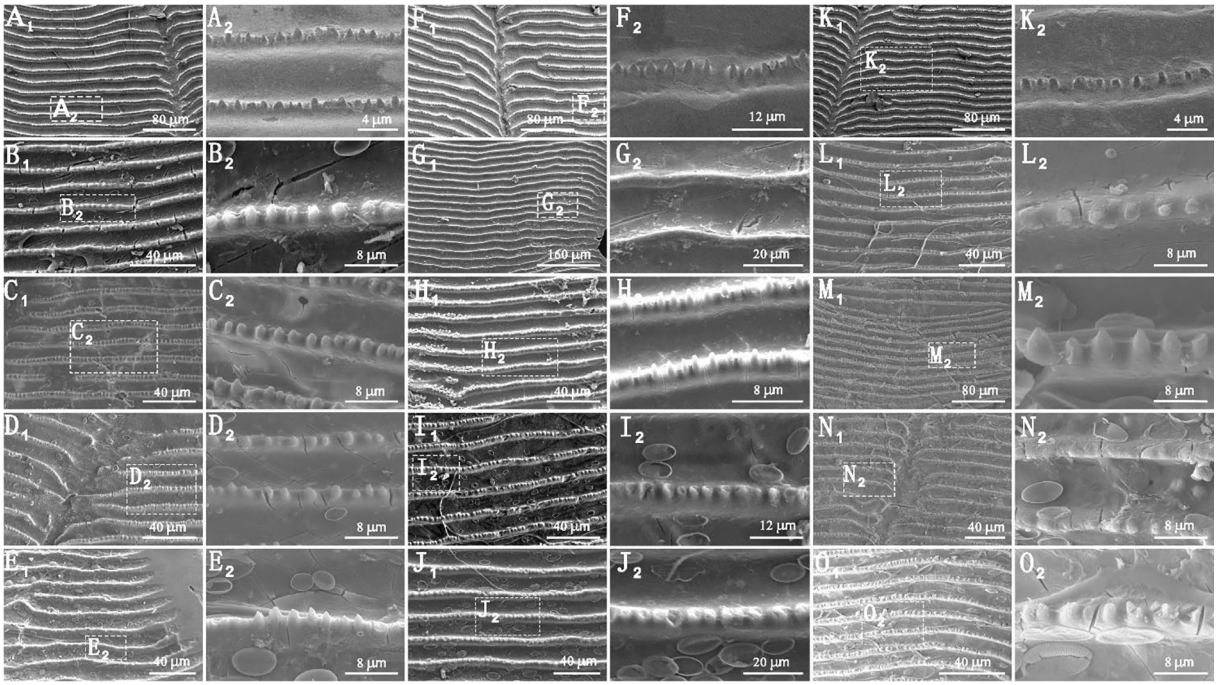

Figure 4

FE-SEM analysis of lepidont ultrastructures in scales from different body regions (caudal, ventral, dorsal). From left to right: FE-SEM images of the lepidont regions in scales from the caudal (tail), ventral (abdomen), and dorsal (back) regions of red seabream (*P.* major). **(A,F,K)** Untreated control scales from the three respective body regions. **(B–E)** Correspond to FE-SEM images of caudal scales subjected to experimental aquaria with pH levels of 7.1, 7.5, 7.7, and 7.9, respectively. **(G–J,L–O)** Also represent FE-SEM observations of ventral scales and dorsal scales under identical pH treatments, respectively. FE-SEM, field emission scanning electron microscopy.

lepidont ultrastructure lacks linear patterns. The authors propose that this divergence arises because lepidonts, composed solely of collagen fiber layers and devoid of calcium salts, are inherently more sensitive to seawater pH fluctuations. In contrast, ctenii are calcified and contain polysaccharides (Fouda, 1979) that stabilize their structure. Collagen, compared with hydroxyapatite (the mineral component of ctenii), demonstrates heightened pH sensitivity due to its organic matrix vulnerability.

The collagen in fish scales is classified as type I collagen (Pulikkottil Rajan, 2024), consisting of two alpha1 chains and one alpha2 chain (Bielajew et al., 2020). This collagen adopts a triple-helical configuration characterized by three polypeptide chains with repeating motifs (Alves et al., 2017). Environmental pH modulates protein hydration through net charge regulation (Hamm, 1986), which subsequently alters collagen's microscopic organization. Within the acidic pH range (3–6), collagen demonstrates enhanced solubility resulting from amplified intermolecular electrostatic repulsion (Damodaran & Parkin, 2017; Pal & Suresh, 2017). However, maximum solubility thresholds vary contingent upon fish species and collagen subtype composition (Damodaran & Parkin, 2017; Pal & Suresh, 2017). Fish scales contain significant quantities of calcium, primarily existing as hydroxyapatite composed principally of calcium (Ca) and phosphorus (P) (Abdullah et al., 2023). Lepidontal composition studies documented calcium-deficient collagenous matrices (Fouda, 1979). Reduced environmental pH may promote physicochemical changes in calcium homeostasis, including hydroxyapatite demineralization or structural reorganization within scales, as the major mechanism for our observed responses of lepidontal/ctenial microstructures to OA (Ocean acidification).

The morphological and ornamentation features of scales in freshwater and marine fish species have been extensively studied (Alkaladi et al., 2013; Harabawy, 2002; Harabawy et al., 2012; Lippitsch, 1993; Mekkawy et al., 1999, 2003; Renjith et al., 2014). Both light microscopy (LM) and scanning electron

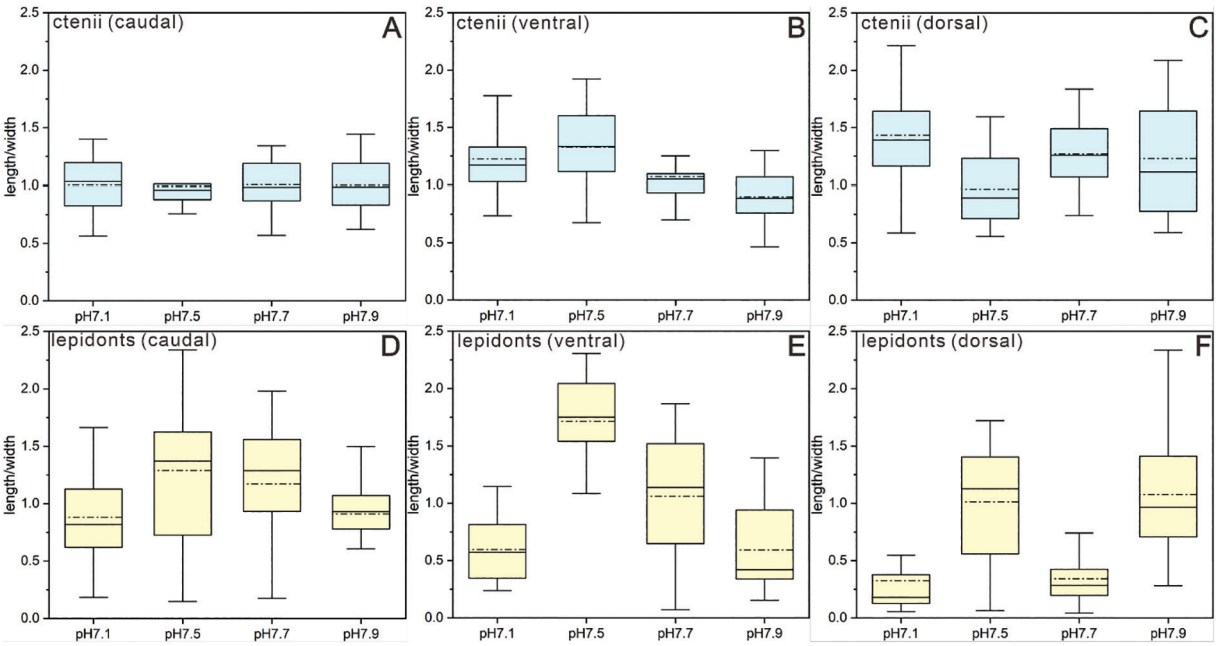

Figure 5

Box plot analysis of the aspect ratios of ctenii and lepidont ultrastructures in scales from different body regions (caudal, ventral, dorsal) under varying pH conditions. **(A–C)** Box plots of ctenii microstructure aspect ratios (length/width) for caudal, ventral, and dorsal scales at pH 7.1, 7.5, 7.7, and 7.9. **(D–F)** Box plots of lepidont microstructure aspect ratios (length/width) for caudal, ventral, and dorsal scales under the different pH conditions. Boxplot elements: Solid line = median; dashed line = mean; box limits = 1st and 3rd quartiles; whiskers = data within 1.5 × interquartile range.

microscopy(SEM) are commonly utilized to analyze scale morphology in environmental studies, enhanced the application of scale morphology in ichthyological research by revealing cryptic structural details (Ibáñez & Jawad, 2018). Fish scales have been established as bioindicators of aquatic ecosystem pollution (Esmaeili et al., 2019; Kaur & Dua, 2012). Our data show that within pH 7.5–7.9, the mean aspect ratio of ventral ctenii and caudal/ventral lepidonts showed a linear decline as pH increased ($r = -0.25$, $p = 0.02$; $r = -0.35$, $p = 0.008$; $r = -0.62$, $p < 0.001$), introducing a semiquantitative model establishing correlations between ocean acidification stress and ultrastructural changes in fish scales.

Ocean acidification presents a growing threat to marine ecosystems globally. A key scientific objective involves identifying reliable bioindicators to monitor the ecological impacts of seawater chemistry alterations for policymakers (Gaylord et al., 2018). Candidate bioindicators for ocean acidification must demonstrate: (1) pH sensitivity, (2) ecological relevance, (3) monitoring feasibility, and (4) socioeconomic importance (Gaylord et al., 2018). Declining populations of hard corals, crustose coralline algae (CCA), and calcifying invertebrates, coupled with proliferating non-calcifying algae and seagrasses, constitute recognized OA bioindicators (Meyer et al., 2015). However, the monitoring scope remains relatively limited, primarily applicable to nearshore and benthic coastal marine environments. Certain benthic algal taxa, widely distributed in shallow photic zones, also represent potential bioindicators of coastal seawater acidification, like the brown alga *Padina pavonica* exhibits sensitivity to both acute and chronic environmental pH fluctuations (Gil-Díaz et al., 2014). Mollusk shells are utilized to monitor acidification in rocky coastal areas due to their occupancy of hard substrates, intertidal pools, and occasionally soft sediments between boulders, spanning the extensive mid-intertidal zone (Marshall et al., 2019). pH ranges were 8.60–5.93 for the acidified sites, with a wide pH gradient. Studies have shown that healthy adult specimens of the pteropod *Limacina helicina* with intact periostraca (the outer organic shell layer) exhibit no dissolution of their shell surfaces even when exposed to aragonite-undersaturated seawater (pH ~ 7.5) (Miller et al., 2023). However, compromised periostraca enables rapid dissolution initiation: under supersaturated conditions (pH ~ 8), shells maintain structural integrity despite experimental abrasion (Miller et al., 2023). Additionally, distinguishing between bioerosion and dissolution by acidified water

in gastropod shells poses significant challenges: shell abrasion can be exacerbated by increased wave action and/or exposure to suspended sediments (Marshall et al., 2019).

Current bioindicators for ocean acidification predominantly consist of benthic organisms or phytoplankton. In contrast, fish, as mobile nektonic species, are widely distributed and exhibit high ecological sensitivity, offering distinct advantages due to their ease of measurement, collection, and application, as well as their widespread distribution. Since different fish species occupy distinct ecological niches across oceanic depths (Sutton, 2013), pelagic fish scales from surface waters act as acidification proxies for the upper water column, whereas demersal taxa reflect bathypelagic acidification trends. We recommend policy integration of scale morphology metrics and standardized assessment protocols to establish acidification monitoring benchmarks, and as semi-quantitative indicators for monitoring ocean acidification. Strategic partnerships with marine industries (e.g., fisheries, tourism sectors) will enable coordinated implementation of acidification mitigation strategies, enhancing ecosystem and socioeconomic resilience (Vasanth et al., 2025).

In addition, the identification of geological acidification is very challenging as its relies on limited sedimentary structures and few geochemical proxies of animal skeletons and there is no reliable paleo-oceanic pH bioindicator for pre-Cenozoic times (Foster et al., 2022). The relative common fossil records of fish scales in sedimentary rocks of Phanerozoic thoroughly validate our proposed proxies to be a potential candidate bioindicator for pH reconstruction of palaeo-oceans (Antczak and Bodzioch, 2018; Cui et al., 2023; Shackleton, 1987).

Acknowledgement

The authors acknowledge the National Science Foundation of China for grants received (42325202; 92155201).

Authors' contributions

Weili Hou: Software; Formal Analysis; Investigation; Writing—original draft; Writing—review & editing; Li Tian: Conceptualization; Writing–original draft, Supervision; Resources; Project Administration; Funding Acquisition; Writing–review & editing. Xin Sun: Experiment; Writing–review & editing, Methodology. Xin Li: Experiment, Writing–review & editing. Xiangming Chen: Writing–review & editing. Haijun Song: Writing–review & editing, Project administration, Methodology, Funding acquisition.

Conflicts of interest

The authors declare that they have no known competing financial interests or personal relationships that could have appeared to influence the work reported in this paper.

Data availability statement

The data that support the findings of this study are all available in the contents of this article.

Declaration of generative AI and c-assisted technologies in the writing process

No.

References

Abdullah, H. Z., Idris, M. I., Te Chuan, L., Dermawan, S. K., & Jaffri, M. Z. (2023). Natural hydroxyapatite from black tilapia fish bones and scales for biomedical applications. In: Wan Kamarul Zaman, W. S. & Nurul, A. A. (eds), Sustainable Material for Biomedical Engineering *Application. Singapore: Springer Nature Singapore*, 107-124. https://doi.org/10.1007/978-981-99-2267-3_6

Alkaladi, A., Harabawy, A. S., & Mekkawy, I. A. (2013). Scale characteristics of two fish species, *Acanthopagrus bifasciatus* (Forsskål, 1775) and *Rhabdosargus sarba* (Forsskål, 1775) from the Red Sea at Jeddah, Saudi Arabia. *Pakistan Journal of Biological Sciences: PJBS, 16*(8), 362–371. https://doi.org/10.3923/pjbs.2013.362.371

Alves, A. L., Marques, A. L., Martins, E., Silva, T. H., & Reis, R. L. (2017). Cosmetic potential of marine fish skin collagen. *Cosmetics, 4*(4), 39. https://doi.org/10.3390/cosmetics4040039

Antczak, M., & Bodzioch, A. (2018). Diversity of fish scales in Late Triassic deposits of Krasiejów (SW Poland). *Paleontological Research, 22*(1), 91–100. https://doi.org/10.2517/2017PR012

Bergstad, O. A. (1991). Distribution and trophic ecology of some gadoid fish of the Norwegian deep: 2. Food-web linkages and comparisons of diets and distributions. *Sarsia, 75*(4), 315–325. https://doi.org/10.1080/00364827.1991.10413456

Bielajew, B. J., Hu, J. C., & Athanasiou, K. A. (2020). Collagen: Quantification, biomechanics and role of minor subtypes

in cartilage. *Nature Reviews Materials, 5*(10), 730–747. https://doi.org/10.1038/s41578-020-0213-1

Cai, L., Wu, X., Dong, Z., Li, X., Yi, S., & Li, J. (2014). Physicochemical responses and quality changes of red sea bream (*Pagrosomus major*) to gum arabic coating enriched with ergothioneine treatment during refrigerated storage. *Food Chemistry*, 160(2014), 82–89. https://doi.org/10.1016/j.foodchem.2014.03.093

Caldeira, K., & Wickett, M. E. (2003). Anthropogenic carbon and ocean pH. *Nature, 425*(6956), 365–365. https://doi.org/10.1038/425365a

Caldeira, K., & Wickett, M. E. (2005) Ocean model predictions of chemistry changes from carbon dioxide emissions to the atmosphere and ocean. *Journal of Geophysical Research*, *110*, 1–12. https://doi.org/10.1029/2004JC002671

Cooley, S. R., & Doney, S. C. (2009). Anticipating ocean acidification's economic consequences for commercial fisheries. *Environmental Research Letters, 4*(2), 024007. https://doi.org/10.1088/1748-9326/4/2/024007

Cui, X., Friedman, M., Yu, Y., Zhu, Y. A., & Zhu, M. (2023). Bony-fish-like scales in a Silurian maxillate placoderm. *Nature Communications, 14*(1), 7622. https://doi.org/10.1038/s41467-023-43557-9

Damodaran, S. & Parkin, K. L. (2017). Amino acids, peptides, and proteins. In: Damodaran, S., Parkin, K. L. & Fennema, O. R. (eds), *Fennema's food chemistry*. Boca Raton: CRC Press, 235–356.

Doney, S. C., Fabry, V. J., Feely, R. A., & Kleypas, J. A. (2009). Ocean acidification: The other CO2 problem. *Annual Review of Marine Science, 1*(1), 169–192. https://doi.org/10.1146/annurev.marine.010908.163834

Echreshavi, S., Al Jufaili, S. M., & Esmaeili, H. R. (2023). Imaging scale surface topography of an endemic cyprinid fish, *Garra sharq* from the Arabian Peninsula: An integrated optical light and scanning electron microscopy approach. *Acta Zoologica, 104*(4), 657–676. https://doi.org/10.1111/azo.12449

Esmaeili, H. R., Zarei, F., Sanjarani Vahed, N., & Masoudi, M. (2019). Scale morphology and phylogenetic character mapping of scale-surface microstructures in *sixteen Aphanius species* (Teleostei: Aphaniidae). *Micron*, *119*(2019), 39–53. https://doi.org/10.1016/j.micron.2019.01.002

Feely, R. A., Alin, S. R., Newton, J., Sabine, C. L., Warner, M., Devol, A., Krembs, C., & Maloy, C. (2010). The combined effects of ocean acidification, mixing, and respiration on pH and carbonate saturation in an urbanized estuary. *Estuarine, Coastal and Shelf Science, 88*(4), 442–449. https://doi.org/10.1016/j.ecss.2010.05.004

Feely, R. A., Doney, S. C., & Cooley, S. R. (2009). Ocean acidification: Present conditions and future changes in a high-CO_2 world. *Oceanography, 22*(4), 36–47. https://www.jstor.org/stable/24861022. https://doi.org/10.5670/oceanog.2009.95

Foster, W. J., Hirtz, J. A., Farrell, C., Reistroffer, M., Twitchett, R. J., & Martindale, R. C. (2022). Bioindicators of severe ocean acidification are absent from the end-Permian mass extinction. *Scientific Reports, 12*(1), 1202. https://doi.org/10.1038/s41598-022-04991-9

Fouda, M. M. (1979). Studies on scale structure in the common goby *Pomatoschistus microps* Krøyer. *Journal of Fish Biology, 15*(2), 173–183. https://doi.org/10.1111/j.1095-8649.1979.tb03581.x

Frimodt, C. (1995). Multilingual illustrated guide to the world's commercial coldwater fish (pp. xix+–244). Oxford.

Fu, J., Chen, C., & Chu, Y. (2019). Spatial–temporal variations of oceanographic parameters in the Zhoushan sea area of the East China Sea based on remote sensing datasets. *Regional Studies in Marine Science*, *28*(2019), 100626. https:// doi. org/ 10.1016/ j. rsma. 2019.100626

Gattuso, J. P., & Hansson, L. (Eds.). (2011). *Ocean acidification*. Oxford University Press.

Gaylord, B., Rivest, E., Hill, T., Sanford, E., Shukla, P., Ninokawa, A., & Ng, G. (2018). *California mussels as bio-indicators of ocean acidification*. California's Fourth Climate Change Assessment.

Gil-Díaz, T., Haroun, R., Tuya, F., Betancor, S., & Viera-Rodriguez, M. A. (2014). Effects of ocean acidification on the brown alga *Padina pavonica*: Decalcification due to acute and chronic events. *Plos One, 9*(9), e108630. https://doi.org/10.1371/journal.pone.0108630

Hamm, R. (1986). Functional properties of the myofibrillar system and their measurements. In (P. J. Bechtel Ed.). *Muscle as food*. Food Science and Technology (pp. 135–191). Academic Press Inc. https://doi.org/10.1016/B978-0-12-084190-5.50009-6

Harabawy, A. S. A. (2002). Biological and taxonomic studies on some fish species of the genus Lethrinus (Family: Lethrinidae) from the Red Sea, Egypt and the genus *Abramis* (Family: Cyprinidae) from the Baltic drainage [Doctoral dissertation, Ph.D. Thesis, Assiut University, Egypt].

Harabawy, A. S., Mekkawy, I. A., & Alkaladi, A. (2012). Identification of three fish species of genus *Plectorhynchus* from the Red Sea by their scale characteristics. *Life Science Journal, 9*(4), 4472–4485. https://doi.org/10.7537/marslsj090412.673

Hutchinson, J. J., & Trueman, C. N. (2006). Stable isotope analyses of collagen in fish scales: Limitations set by scale architecture. *Journal of Fish Biology, 69*(6), 1874–1880. https://doi.org/10.1111/j.1095-8649.2006.01234.x

Ibáñez, A. L., & Jawad, L. A. (2018). Morphometric variation of fish scales among some species of rattail fish from New Zealand waters. *Journal of the Marine Biological Association of the United Kingdom, 98*(8), 1991–1998. https://doi.org/10.1017/S0025315418000024

Iglesias-Rodriguez, M. D. (2012). Ocean acidification. In: Orcutt, J. (ed.), *Earth system monitoring: Selected entries from the encyclopedia of sustainability science and technology*.

Berlin: Springer, 269–289. https://doi.org/10.1007/978-1-4614-5684-1_12

Kaur, R., & Dua, A. (2012). Fish scales as indicators of wastewater toxicity from an international water channel Tung Dhab drain. *Environmental Monitoring and Assessment, 184*(5), 2729–2740. https://doi.org/10.1007/s10661-011-2147-y

Kaur, K., Kaur, R., & Kaur, A. (2016). Surface microstructural features of scales in relation to toxic stress of Basic Violet-1. *Environmental Science and Pollution Research International, 23*(2), 1173–1182. https://doi.org/10.1007/s11356-015-5374-x

Khanna, D. R., Sarkar, P., Gautam, A., & Bhutiani, R. (2007). Fish scales as bio-indicator of water quality of River Ganga. *Environmental Monitoring and Assessment, 134*(1–3), 153–160. https://doi.org/10.1007/s10661-007-9606-5

Lanzing, W. J. R., & Higginbotham, D. R. (1974). Scanning microscopy of surface structures of *Tilapia mossambica* (Peters) scales. *Journal of Fish Biology, 6*(3), 307–310. https://doi.org/10.1111/j.1095-8649.1974.tb04547.x

Lippitsch, E. (1993). A phyletic study on lacustrine haplochromine fishes (*Perciformes*, Cichlidae) of East Africa, based on scale and squamation characters. *Journal of Fish Biology, 42*(6), 903–946. https://doi.org/10.1111/j.1095-8649.1993.tb00399.x

Liu, W. T., & Xie, X. (2017). Space observation of carbon dioxide partial pressure at ocean surface. *IEEE Journal of Selected Topics in Applied Earth Observations and Remote Sensing, 10*(12), 5472–5484. https://doi.org/10.1109/JSTARS.2017.2766138

Li, D., Wang, B., Jin, H., Miao, Y., Sun, Q., Lin, H., Li, H., Liu, Q., Zhou, F., & Chen, J. (2024). Decoupling of high-resolution surface pH and DO reveals temporal algal bloom dynamics on the East China Sea. *Water Research*, *261*(2024), 122030. https:// doi. org/ 10.1016/ j. watres. 2024.122030

Marshall, D. J., Abdelhady, A. A., Wah, D. T. T., Mustapha, N., Gödeke, S. H., De Silva, L. C., & Hall-Spencer, J. M. (2019). Biomonitoring acidification using marine gastropods. *Science of the Total Environment*, *692*(2019), 833–843. https:// doi. org/ 10.1016/ j. scitotenv. 2019.07.041

Mekkawy, I.A.A., Mahmoud, U.M., & Harabawy, A.S.A. (2003). Identification of four Labeo fish species from the Nile, Egypt by their scale characteristics and scanning electron *microscopy. Journal of Union of Arab Biologists Cairo. A, Zoology, 19*(A):81-104.

Mekkawy, I.A.A., Shehata, S.M.A., Saber, S.A. and Osman, A.G.M. (1999). Scale characteristics of five species of genus *Epinephelus* (Family: Serranidae) from the Red Sea Egypt. *Journal-Egyptian German Society of Zoology, 30*(B): 71–102.

Meyer, F.W., Cardini, U., Wild, C. (2015). Ocean Acidification and Related Indicators. In: Armon, R., Hänninen, O. (eds) *Environmental Indicators*. Springer, Dordrecht. https://doi.org/10.1007/978-94-017-9499-2_41

Miller, M. R., Oakes, R. L., Covert, P. A., Ianson, D., & Dower, J. F. (2023). Evidence for an effective defense against ocean acidification in the key bioindicator pteropod *Limacina helicina*. *ICES Journal of Marine Science, 80*(5), 1329–1341. https://doi.org/10.1093/icesjms/fsad059

Ní Longphuirt, S., Stengal, D., O'dowd, C., & McGovern, E. (2010). Ocean acidification: An emerging threat to our marine environment. *Marine Institute*.

NOAA. (2025). Ocean acidification. National Oceanic and Atmospheric Administration. https://www.noaa.gov/education/resource-collections/ocean-coasts/ocean-acidification

Orr, J. C., Fabry, V. J., Aumont, O., Bopp, L., Doney, S. C., Feely, R. A., Gnanadesikan, A., Gruber, N., Ishida, A., Joos, F., Key, R. M., Lindsay, K., Maier-Reimer, E., Matear, R., Monfray, P., Mouchet, A., Najjar, R. G., Plattner, G. K., Rodgers, K. B., … Yool, A. (2005). Anthropogenic ocean acidification over the twenty-first century and its impact on calcifying organisms. *Nature, 437*(7059), 681–686. https://doi.org/10.1038/nature04095

Pal, G. K., & Suresh, P. V. (2017). Comparative assessment of physico-chemical characteristics and fibril formation capacity of thermostable carp scales collagen. *Materials Science and Engineering: C, 70*(Pt–1), 32–40. https://doi.org/10.1016/j.msec.2016.08.047

Pulikkottil Rajan, D. (2024). Derivatives of Structural Proteins. In: Raman, M., Sasidharan, A., Sabu, S. & Pulikkottil Rajan, D. (eds), *Fish structural proteins and its derivatives: Functionality and applications. Singapore: Springer Nature Singapore*, 73–105.

Renjith, R. K., Jaiswar, A. K., Chakraborty, S. K., Jahageerdar, S., & Sreekanth, G. B. (2014). Application of scale shape variation in fish systematics-an illustration using six species of the family Nemipteridae (Teleostei: Perciformes). *Indian Journal of Fisheries, 61*(1), 88–92. https://doi.org/10.21077/

Ridgwell, A., & Schmidt, D. N. (2010). Past constraints on the vulnerability of marine calcifiers to massive carbon dioxide release. *Nature Geoscience, 3*(3), 196–200. https://doi.org/10.1038/ngeo755

Rishi, K. K., & Jain, M. (1998). Effect of toxicity of cadmium on scale morphology in *Cyprinus carpio* (Cyprinidae). *Bulletin of Environmental Contamination and Toxicology, 60*(2), 323–328. https://doi.org/10.1007/s001289900629

Sabine, C. L., Feely, R. A., Gruber, N., Key, R. M., Lee, K., Bullister, J. L., Wanninkhof, R., Wong, C. S., Wallace, D. W. R., Tilbrook, B., Millero, F. J., Peng, T.-H., Kozyr, A., Ono, T., & Rios, A. F. (2004). The oceanic sink for anthropogenic CO2. *Science, 305*(5682), 367–371. https://doi.org/10.1126/science.1097403

Sarker, S. A., Satoh, S., & Kiron, V. (2005). Supplementation of citric acid and amino acid-chelated trace element to develop environment-friendly feed for red sea bream, *Pagrus major*. *Aquaculture, 248*(1–4), 3–11. https://doi.org/10.1016/j.aquaculture.2005.04.012

Shackleton, L. Y. (1987). A comparative study of fossil fish scales from three upwelling regions. *South African Journal of Marine Science, 5*(1), 79–84. https://doi.org/10.2989/025776187784522270

Silverman, J., Lazar, B., Cao, L., Caldeira, K., & Erez, J. (2009). Coral reefs may start dissolving when atmospheric CO2 doubles. *Geophysical Research Letters, 36*,1-5(2009). https://doi.org/10.1029/2008GL036282

Solomon S, Qin D, Manning M. Technical summary. In: Solomon S, Qin D, Manning M, Marquis M, Averyt K, Tignor MMB, Miller HL, Chen ZL, editors. Climate change 2007. The physical science basis. Contribution of working group i to the fourth assessment report of the intergovernmental panel on climate change. United Kingdom and New York, NY, USA: Cambridge University Press, Cambridge; 2007. p. 19–91.

Tignor, & H. L. Miller (Eds.), *Climate change 2007: The physical science basis. Contribution of working group I to the fourth assessment report of the intergovernmental panel on climate change*.

Sutton, T. T. (2013). Vertical ecology of the pelagic ocean: Classical patterns and new perspectives. *Journal of Fish Biology, 83*(6), 1508–1527. https://doi.org/10.1111/jfb.12263

Vasanth, K., Kishore, R. K., Sugumaran, V., Krishnamoorthy, R., Ramdas, R., & Tadepalli, S. K. (2025). Multi-variate hybrid modeling for pacific ocean acidification: predicting future pH trends and analyzing key biogeochemical drivers. CSI *Transactions on ICT, 13*(1), 99-116. https:// doi. org/ 10.1007/ s40012- 024- 00406- 4 11

Wainwright, D. K. & Lauder, G. V. 2018. Mucus matters: the slippery and complex surfaces of fish. In: Gorb, S. N. & Gorb, E. V. (eds), *Functional Surfaces in Biology III: Diversity of the Physical Phenomena.* Cham: Springer International Publishing, 223-246. https://doi.org/10.1007/978-3-319-74144-4_10

Wang, Q., Bai, P., Yang, J., Li, P., Yu, C., Wu, Q., Ruan, Z., & Li, B. (2025). Seafloor temperature variability in the Zhoushan Archipelago: Patterns and mechanisms. *Estuarine, Coastal and Shelf Science, 320*, 109298. https://doi.org/10.1016/j.ecss.2025.109298

Weiner, S., & Wagner, H. D. (1998). The material bone: Structure-mechanical function relations. *Annual Review of Materials Science, 28*(1), 271–298. https://doi.org/10.1146/annurev.matsci.28.1.271

Xiao, T., Feng, J., Qiu, Z., Tang, R., Zhao, A., Wong, K., Tsou, J. Y., & Zhang, Y. (2024). Remote-sensing estimation of upwelling-frequent areas in the adjacent waters of Zhoushan (China). *Journal of Marine Science and Engineering, 12*(7), 1085. https://doi.org/10.3390/jmse12071085

Zeebe, R. E., Zachos, J. C., Caldeira, K., & Tyrrell, T. (2008). Carbon emissions and acidification. *Science, 321*(5885), 51–52. https://doi.org/10.1126/science.1159124

Zylberberg, L. (1988). Ultrastructural data on the scales of the dipnoan *Protoptems annectens* (Sarcopterygii, Osteichthyes). *Journal of Zoology, 216*(1), 55–71. https://doi.org/10.1111/j.1469-7998.1988.tb02415.x

Zylberberg, L. (2004). New data on bone matrix and its proteins. *Comptes Rendus Palevol, 3*(6–7), 591–604. https://doi.org/10.1016/j.crpv.2004.07.012

Zylberberg, L., & Nicolas, G. (1982). Ultrastructure of scales in a teleost (*Carassius auratus* L.) after use of rapid freeze-fixation and freeze-substitution. *Cell and Tissue Research, 223*(2), 349–367. https://doi.org/10.1007/BF01258495